

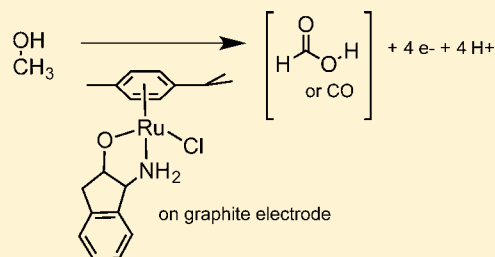
Electrooxidation of Alcohols Catalyzed by Amino Alcohol Ligated Ruthenium Complexes

Kristen R. Brownell, Charles C. L. McCrory, Christopher E. D. Chidsey, Richard H. Perry, Richard N. Zare, and Robert M. Waymouth*

Department of Chemistry, Stanford University, Stanford, California 94305-5080, United States

S Supporting Information

ABSTRACT: Ruthenium transfer hydrogenation catalysts physisorbed onto edge-plane graphite electrodes are active electrocatalysts for the oxidation of alcohols. Electrooxidation of CH₃OH (1.23 M) in a buffered aqueous solution at pH 11.5 with [(η⁶-*p*-cymene)(η²-*N,O*-(1*R*,2*S*)-*cis*-1-amino-2-indanol)]-Ru^{II}Cl (**2**) on edge-plane graphite exhibits an onset current at 560 mV vs NHE. Koutecky–Levich analysis at 750 mV reveals a four-electron oxidation of methanol with a rate of 1.35 M⁻¹ s⁻¹. Mechanistic investigations by ¹H NMR, cyclic voltammetry, and desorption electrospray ionization mass spectrometry indicate that the electrooxidation of methanol to generate formate is mediated by surface-supported Ru–oxo complexes.



INTRODUCTION

Alcohols are attractive chemical fuels for fuel cells due to their high energy densities, established production and distribution infrastructure, and ability to be derived from renewable resources.^{1–3} However, even the most highly optimized alcohol electrooxidation catalysts suffer from kinetic limitations that require high overpotentials to achieve reasonable rates.^{2–11} Polypyridyl ruthenium–oxo complexes are among the most highly developed class of alcohol electrooxidation complexes^{12–14} but require relatively large overpotentials.^{13,15–19}

We targeted transfer hydrogenation (TH) catalysts^{20,21} as a potentially attractive class of candidates for alcohol electrooxidation catalysts, since catalytic transfer hydrogenation involves the reversible oxidation of alcohols with ketones as terminal oxidants. In a typical transfer hydrogenation, an alcohol serves as a hydrogen donor to reduce a ketone (Scheme 1). The chemical reversibility of TH reactions suggests that the catalysts mediating these transformations are operating close to their reversible redox potentials and thus are promising candidates for reversible alcohol electrooxidation catalysts. Transfer hydrogenation of ketones by alcohols with cymene Ru complexes was reported by Noyori and Ikariya.^{21,22} Mechanistic studies^{21–26} indicate that the concerted dehydrogenation of alcohols by the Ru amide **A** generates a ketone and the Ru–H **B**, which in turn can reduce a ketone to regenerate **A** (Scheme 1).

Due to their promising reactivity in transfer hydrogenation, we investigated complexes **1** and **2** as molecular electrocatalysts for alcohol oxidation (Figure 1). Complex **2**, derived from [Ru(*p*-cymene)Cl₂]₂ and (1*R*,2*S*)-*cis*-1-amino-2-indanol, is more active than the Ru–Cl complex **1**^{27,28} and exhibits turnover frequencies of up to 540 h⁻¹ for transfer hydrogenations of ketones with 2-propanol at room temperature with 2.5 mol % KOH,²⁸ nearly 60 times faster than complex **1**.^{27,28}

Scheme 1. Transfer Hydrogenation of Ketones by Alcohols

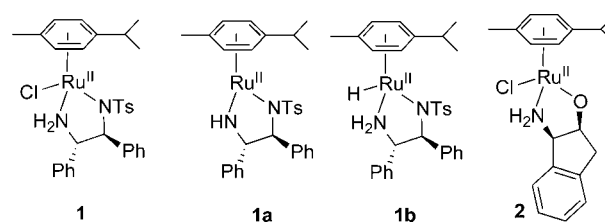
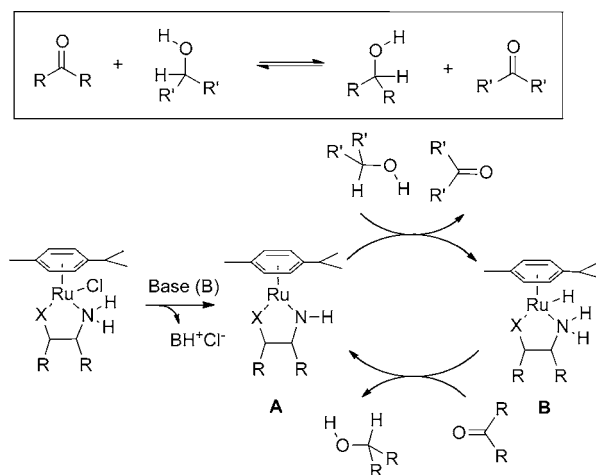


Figure 1. Cymene Ru complexes.

Herein we show that the complexes **1a** and **2** are active for the electrocatalytic oxidation of alcohols when supported on

Received: June 17, 2013

Published: September 17, 2013

edge-plane graphite (EPG) electrodes in basic aqueous solution. When physisorbed onto EPG electrodes, complex **2** exhibits rapid rates for methanol oxidation by four electrons at 750 mV vs NHE and pH 11.5. The structurally similar complex **1** also exhibits rapid rates for 2-propanol electrooxidation, albeit slower than those for **2**. Proton NMR, cyclic voltammetry, and desorption electrospray ionization mass spectrometry studies on the electrode surface before and after catalysis indicate that the four-electron-oxidation product of methanol is formate.

RESULTS AND DISCUSSION

Synthesis. Complexes **1** and **1a,b** were prepared as previously described.²² Attempts to prepare the Ru–Cl complex **2**^{28,29} analogously to **1**²² were unsuccessful, resulting in a mixture of the ruthenium chloride and hydride species. Instead, **2** was prepared by the dropwise addition of a THF solution of [(*p*-cymene)RuCl]₂ to a THF solution of the sodium salt of (1*R*,2*S*)-*cis*-1-amino-2-indanol at –78 °C. Recrystallization from diethyl ether/pentane at reduced temperature afforded **2** in analytically pure form.

Transfer Hydrogenation. Catalytic transfer hydrogenations of ketones typically employ 2-propanol or formate as a hydrogen donor. While methanol has been investigated previously²² as a hydrogen donor for the transfer hydrogenation of ketones, it is less effective than 2-propanol.³⁰ To compare the reactivities of the two alcohols with complexes **1** and **2**, the catalytic transfer hydrogenation of acetophenone by both methanol and 2-propanol was performed to compare the relative reactivity of the diamide **1a** and the Ru chlorides **1** and **2** (Scheme 2 and Table 1). While **1a** does not require a base for

Scheme 2. Transfer Hydrogenation of Acetophenone (1.22 M) with (a) 2-Propanol and (b) Methanol Employing 1a, 1, and 2

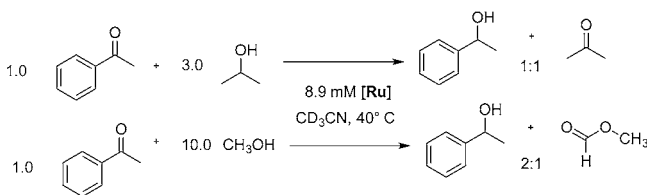


Table 1. Initial Turnover Frequencies for Transfer Hydrogenation Catalyzed by 1, 1a, and 2^a

catalyst	alcohol	concn of sodium alkoxide (M)	TOF _i (h ⁻¹)
1a	methanol	0.17 (methoxide)	6.5
1	methanol	0.17 (methoxide)	8.5
2	methanol	0.17 (methoxide)	21
1a	2-propanol	0.035 (isopropoxide)	18
1	2-propanol	0.035 (isopropoxide)	26
2	2-propanol	0.035 (isopropoxide)	113

^aReactions performed under inert conditions at 40 °C in CD₃CN with 1.22 M acetophenone, 3.66 M 2-propanol or 9.27 M methanol, and 8.9 mM catalyst with *p*-xylene as an internal standard. TOF_i = (mmol of acetophenone consumed)/(mmol catalyst time), measured at 0.25 h.

activity, reactions with methanol and 2-propanol were carried out in the presence of the alkoxide to provide comparable experimental conditions. The reactions were monitored by ¹H NMR, and initial turnover frequencies were calculated from the

slopes of the first several points of the acetophenone conversion vs time plots.

The catalytic transfer hydrogenation of acetophenone with methanol in the presence of complexes **1a**, **1**, and **2** affords 1-phenylethanol and methyl formate in a ratio of 2:1, indicating that methanol provides two reducing equivalents. Methyl formate is observed as the only product of methanol dehydrogenation via ¹H NMR and GC-MS. The oxidation of methanol to methyl formate^{31–33} by Ru(II) complexes has been observed previously and likely proceeds by the initial dehydrogenation of methanol to formaldehyde, followed by condensation with methanol to the acetal and subsequent dehydrogenation.^{31–36}

These results reveal that the initial rates for the TH of acetophenone were faster for 2-propanol than for methanol and that for both alcohols the catalyst derived from the Ru–Cl complex **2**, derived from the amino alcohol ligand, was more active than that derived from the diamide **1** or **1a**. The latter result is consistent with the reports of Wills²⁸ and Blacker³⁰ that catalysts derived from amino alcohol ligands are more active for transfer hydrogenation than those from diamide ligands.

Electrocatalytic Alcohol Oxidation. Electrocatalytic oxidation of methanol and 2-propanol were investigated by rotating disk electrode (RDE) voltammetry with samples of the Ru–Cl complex **2** and the Ru–amide complex **1a** deposited onto edge-plane graphite (EPG) electrodes (Table 2, Figure 2). Electrochemical measurements were recorded with a potentiostat using an MSR rotator, an auxiliary Pt-wire electrode, and a Ag/AgCl/KCl (sat) reference electrode in aqueous solutions of 0.01 M phosphate and 0.1 M sodium perchlorate. The pH was adjusted by addition of 1.0 M solutions of either NaOH or HClO₄.

We investigated the electrocatalytic oxidation of both methanol and 2-propanol with the amino alkoxide Ru–Cl complex **2**. The cyclic voltammogram (CV) of **2** physisorbed onto EPG in a 0.1 M sodium perchlorate solution at pH 5.4 under an N₂ atmosphere exhibits a quasi-reversible oxidation at E_{1/2} = 540 mV vs NHE (ΔE_{p-p} = 460 mV) under a nitrogen atmosphere, which is attributed to the Ru^{II/III} couple (Figure S4a, Supporting Information).^{12,37,38} Plots of both the anodic and cathodic peak currents as a function of scan rate are linear, confirming that the electroactive species is surface adsorbed (Figure S4b–d, Supporting Information). A surface coverage of 2.14 × 10⁻¹⁰ mol/cm² of electroactive Ru on the EPG electrode was estimated by integration of the area of the Ru^{II/III} redox peak at pH 5.4. CVs obtained at pH values from pH 2.28 to 11.75 revealed that the anodic peak shifts to more negative potentials with increasing pH at –68 mV per pH unit (Figure S5, Supporting Information).

Electrocatalytic oxidation of methanol catalyzed by **2** was investigated by RDEV in 0.1 M sodium perchlorate aqueous solution with 0.01 M phosphate buffer. When the Ru–Cl **2** is adsorbed onto an edge-plane graphite electrode in 1.23 M methanol solution at pH 11.5, an electrocatalytic current is observed with an onset potential of 560 mV vs NHE (Figure 2a). Analysis of the current as a function of rotation rate (400–3000 rpm, Figure S4) by Koutecký–Levich analysis³⁹ provides estimates of both the kinetic rate constant and the number of electrons involved in the electrocatalytic process. Plots of *i*(*E*)⁻¹, the inverse of the current measured at a constant potential *E* = 750 mV vs NHE, as a function of ω^{-1/2} yield *i*_k(*E*)⁻¹ as the intercept (Figure 2b).³⁹ This kinetic current was

Table 2. Electrocatalytic Alcohol Oxidation by Complexes **2** and **1a** on EPG Electrodes

complex	coverage 10^{-10} mol/cm ²	E_{pa} , mV (pH)	alcohol	pH	n	i_{K} , μA	k , $\text{M}^{-1} \text{s}^{-1}$
2	2.1	770 (5.4)	MeOH	11.5	4	14.9 ^a	1.35
2	2.1		ⁱ PrOH	11.5	2	84.0 ^a	13.9
1a	2.2	1040 (5.96)	ⁱ PrOH	11.5	2	19.5 ^b	2.01
1a	2.2		ⁱ PrOH	5.96	2	38.9 ^c	10.2

^a $E = 750$ mV vs NHE. ^b $E = 650$ mV vs NHE. ^c $E = 1.4$ V vs NHE.

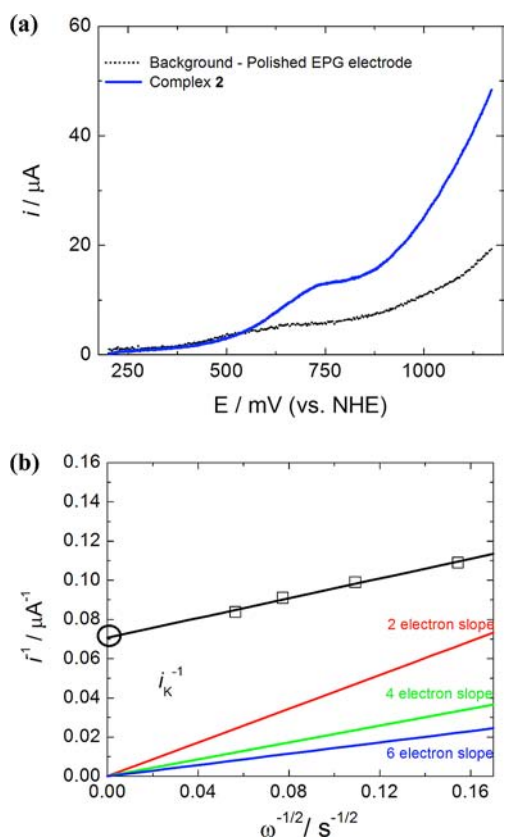
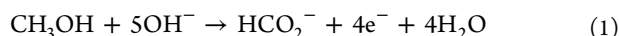


Figure 2. (a) Rotating disk electrode voltammogram of **2** (blue) physisorbed onto EPG in a 1.23 M MeOH aqueous solution at 3000 rpm. The onset of electrocatalytic current (blue) appears at 560 mV over background current (black) of a polished EPG surface in the same solution. Conditions: supporting electrolyte 0.1 M NaClO₄, 0.01 M phosphate buffer, pH 11.5, scan rate 100 mV/s, N₂ atmosphere. (b) Koutecky–Levich plot of the inverse of the plateau current measured at 750 mV vs NHE as a function of (rotation rate)^{-1/2}. The colored lines give the calculated responses for a diffusion-controlled oxidation of methanol by two (red), four (green), and six (blue) electrons.

determined to be $i_{\text{K}}(E) = 14.9 \mu\text{A}$ ($85.1 \mu\text{A cm}^{-2}$). The plot of the inverse currents is parallel to the inverse theoretical Levich current³⁹ calculated with $n = 4$ (Figure 2b), indicative of a four-electron oxidation of methanol to either formate or carbon monoxide (eq 1). This analysis yields a rate constant of $k = 1.35$



$\text{M}^{-1} \text{s}^{-1}$ and a turnover frequency of approximately one methanol/s for the electrocatalytic oxidation of methanol by the amino alcohol complex **2** at 750 mV vs NHE.

Electrooxidation of 2-propanol by **2** exhibited an onset potential of 500 mV vs NHE at pH 11.5. Koutecky–Levich analysis at 650 mV vs NHE is consistent with a two-electron oxidation at a rate of 15.8 electrons/s, corresponding to a rate

constant of $k = 13.9 \text{ M}^{-1} \text{ s}^{-1}$, considerably faster than methanol electrooxidation under similar conditions (Table 1 and Figure S12 (Supporting Information)).

Electrooxidation of 2-propanol with diamide **1a** displayed an onset of electrocatalytic current at 603 mV vs NHE, pH 11.5 (Figure S10, Supporting Information). The rate of 2-propanol electrooxidation by the diamide **1a** was considerably slower than that by the amino alcohol complex **2** ($k = 2.01$ vs $13.9 \text{ M}^{-1} \text{ s}^{-1}$, respectively; Table 2). These relative rates observed in the electrocatalytic alcohol oxidation (Table 2) mirror the trends observed in the catalytic transfer hydrogenation reactions (Table 1):²⁸ complex **2** exhibits faster rates than complex **1a**, and the transfer hydrogenation of acetophenone with 2-propanol is considerably faster than that with methanol.^{22,40} These data provide strong if indirect support that the bidentate ligands remain coordinated to Ru during electrocatalysis. This conclusion is also supported by control experiments, which showed that $[\text{Ru}(p\text{-cymene})\text{Cl}_2]_2$, lacking the bidentate ligands, is not an effective electrocatalyst for 2-propanol oxidation under similar conditions (Figures S15–S17, Supporting Information).

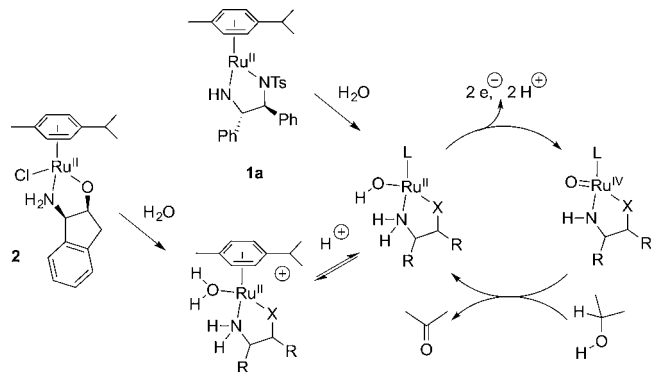
The results of the electrocatalytic experiments show that the molecular Ru cymene complexes **1a** and **2** mediate the electrocatalytic oxidation of aliphatic alcohols at fast rates, albeit at relatively high potentials. The rate constants for methanol and 2-propanol oxidation (650–750 mV vs NHE, pH 11.5) correspond to turnover frequencies of approximately 1 MeOH s⁻¹ and 8 ⁱPrOH s⁻¹. These rates are attractive for fuel cell applications and are comparable to those reported for MeOH electrooxidation with Pd nanoparticle catalysts (1.1 mA/ μg Pd, ~ 0.3 MeOH s⁻¹)⁴¹ but lower than that reported for supported Ni catalysts ($k = 7.4 \times 10^4 \text{ M}^{-1} \text{ s}^{-1}$).^{42,43} For molecular Ru electrocatalysts, rate constants for alcohol electrooxidation range from $k = 0.03$ to $6.6 \times 10^3 \text{ M}^{-1} \text{ s}^{-1}$, depending on the alcohol and the coordination geometry at Ru.^{13,15–19,38,44–50} For example, the Ru–oxo complex $[\text{Ru}^{\text{IV}}(\text{trpy})(\text{phen})\text{O}]^{2+}$ when adsorbed onto a carbon paste electrode electrooxidizes methanol at $0.030 \text{ M}^{-1} \text{ s}^{-1}$ at 0.285 V vs SSCE at pH 13, an overpotential of 1.1 V.¹⁵ The related $[\text{Ru}^{\text{IV}}(\text{bpy})_2(\text{py})\text{O}]$ complex oxidizes methanol with a rate constant of $3.5 \times 10^{-4} \text{ M}^{-1} \text{ s}^{-1}$ at 0.99 V vs SCE (1.23 V vs NHE).⁵¹ Faster rates were reported for methanol electrooxidation with $[\text{Ru}^{\text{V}}[\text{bis}(2\text{-pyridylmethyl})\text{ethylenediamine}]\text{Cl}(\text{O})]$ ($k = 6.6 \times 10^2 \text{ M}^{-1} \text{ s}^{-1}$ at 1.3 V vs SCE; 1.54 V vs NHE)¹⁶ or $[\text{Ru}^{\text{IV}}(\text{dc bpy})_2(\text{O})_2]^{2+}$ (dc bpy = 6,6'-dichloro-2,2'-bipyridine) ($k = 3.3 \text{ M}^{-1} \text{ s}^{-1}$ at 1.39 V vs NHE).¹⁷

The onset of electrocatalytic current for methanol oxidation by **2** reported here occurs at 560 mV vs NHE (pH 11.5, Figure 2a), over 1000 mV positive of the thermodynamic potential of methanol oxidation to formate.⁵² These values are more positive than that reported for Pd nanoparticle catalysts (-0.150 V vs Ag/AgCl/saturated KCl, 50 mV vs NHE; pH 14.4)⁴¹ but comparable to those of other supported or solution-phase molecular electrocatalysts based on Ru,^{13,15–19,53–55} Ni,^{42,43} or Rh.^{9,10}

Proposed Electrocatalytic Mechanism. Transfer hydrogenation catalysts such as complexes **1** and **2** were targeted as promising electrooxidation catalysts, as they mediate the reversible oxidation of alcohols and reduction of ketones by Ru–H and Ru–amide intermediates. The results of our electrocatalytic experiments in water suggest that the electrocatalytic oxidation of methanol and 2-propanol proceed by an alternative mechanism. The electrocatalytic rate (ca. 1 s^{-1}) for methanol oxidation by **2** is much faster than the chemical rate of transfer hydrogenation (ca. 21 h^{-1}) at room temperature. In addition, the potentials at which electrooxidation occurs (650–750 mV vs NHE) are more positive than those expected for Ru–H intermediates.^{56,57} The irreversible oxidation of the Ru–H complex **1b** measured in CH_3CN occurs at -243 mV vs $\text{Cp}_2\text{Fe}^{+/0}$ (Figure S18, Supporting Information). While transfer hydrogenation is known to proceed in water with complexes **1**,⁵⁸ water reacts rapidly with the Ru–amide **1a** to generate a Ru–hydroxo complex (Figure S19, Supporting Information).⁵⁸ These data imply that the electrocatalytic mechanism is not mediated by ruthenium hydrides but more likely by Ru–hydroxo or Ru–oxo complexes.^{12,19,44–46,59,60}

Shown in Scheme 3 is a proposed catalytic mechanism where aqutation of the Ru cymene precursors generates Ru–OH

Scheme 3. Proposed Mechanism for Electrocatalytic Alcohol Oxidation Involving Ru(IV)–Oxo Intermediates^a



^aL = cymene, solvent, or EPG surface.

intermediates (or Ru–OH₂ intermediates, depending on the pH), which under relatively high potentials and basic

conditions would be expected to generate Ru–oxo intermediates (which may or may not retain the arene ligand). Related arene Ru=O intermediates have been proposed to mediate the oxidation of alcohols.^{61,62}

The voltammetry of complexes **1a** and **2** is consistent with this hypothesis, as the anodic peaks in the CVs of **1a** and **2** physisorbed on EPG are dependent upon pH and exhibit Nernstian responses of ca. -59 mV per pH unit, indicative of a proton-coupled electron transfer. Such behavior is typical of Ru–OH₂/Ru–OH/Ru=O redox processes.^{12,18,38,44–47,49,51,63,64} Moreover, the overpotentials calculated (approximately 1 V) are consistent with those observed for other electrocatalytic alcohol oxidations proposed to occur by Ru=O intermediates.^{13,63}

To provide evidence for this proposed mechanism, we employed desorption electrospray ionization mass spectrometry (DESI)^{65–67} to examine species on the electrode surfaces (Figure 3). The development of ambient ionization methods in the past decade has provided new strategies to detect reactive intermediates in solution using mass spectrometry (MS).⁶⁵ DESI, a recently developed ionization method, requires little sample preparation and can be carried out in an open environment.^{65–67} In a DESI experiment, charged droplets in a stream of gas are sprayed on a surface containing a deposited analyte and extract analyte molecules from the surface into secondary microdroplets from which gas-phase ions are formed.⁶⁸ By addition of reagents to the DESI spray, one can perform reactions with compounds adsorbed onto surfaces, intercept short-lived intermediates, and monitor reaction products in real time.⁶⁸ Recently, nano-DESI was employed to study reactions on electrode surfaces,⁶⁹ indicating the power of ambient mass spectrometric techniques in probing electrochemical processes. Here we apply DESI to characterize species after RDE electrocatalysis. These results demonstrate that DESI is a powerful technique to study electrode surfaces, as the measurement can be performed rapidly (<5 min including any instrument preparation time) and can help identify reactive intermediates, including those present in low abundance.

An initial DESI experiment was carried out by depositing complex **2** on edge-plane graphite from an acetone solution and subsequently analyzing the surface species by spraying methanol onto the electrode. The electrode was affixed to a glass slide, and methanol (degassed via sparging with argon) was sprayed onto the surface by a DESI source (0 kV spray

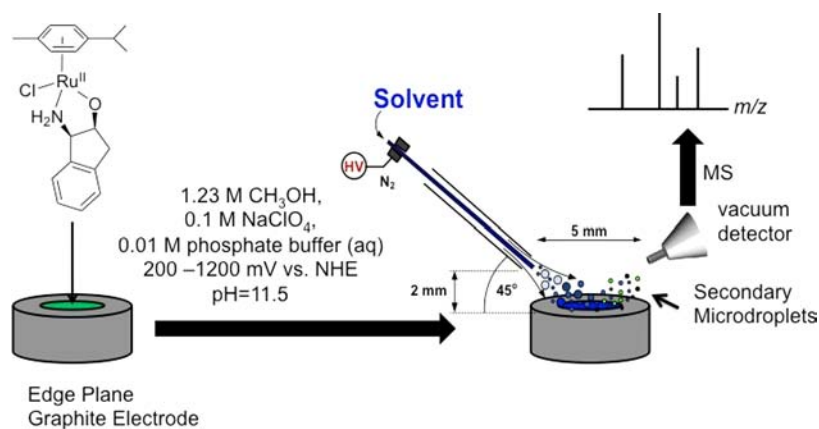


Figure 3. Schematic of DESI experiment to detect species present after electrocatalysis with **2** ($3 \times 2\ \mu\text{L}$ of a 10^{-2} M solution in acetone deposited on edge-plane graphite) using CH_3OH infused at $5\ \mu\text{L}\ \text{min}^{-1}$ (N_2 flow rate $0.6\ \text{L}\ \text{min}^{-1}$).

voltage). The DESI spectrum of complex **2** supported on EPG (Figure 4a) shows several species, including the Ru–Cl cation

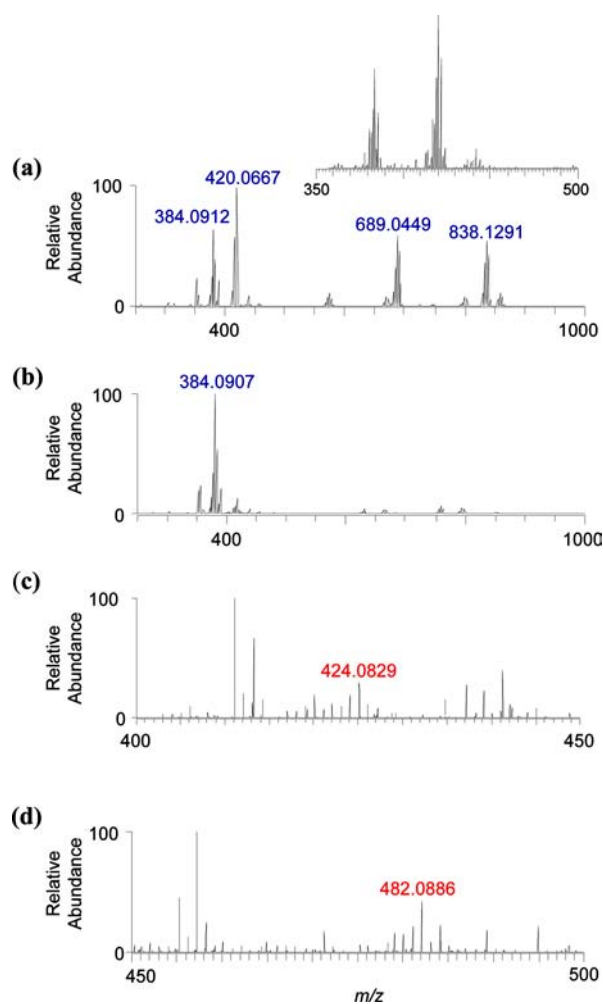


Figure 4. DESI mass spectra of (a) complex **2** supported on an EPG electrode and (b) **2**/EPG following electrocatalysis of methanol. The peak at m/z 420.0677 decreases in abundance and m/z 384.0911 becomes the predominant species. DESI mass spectra showing (c) the peak at m/z 424.0829 and (d) the peak at m/z 482.0886.

2^+ (m/z 420.0667), species $2a^+$ at (m/z 384.0907), the cationic dimer $[(p\text{-cymene})\text{RuCl-Ru}(\text{Cl})_2(p\text{-cymene})]^+$ (m/z 576.9340), and the dimer $[2+2]^+$ (m/z 838.1272). The ions observed at m/z 384.0907 and 420.0667 provide evidence that the Ru–Cl complex **2** remains intact when supported on edge-plane graphite electrodes. These species were observed

previously³¹ in a DESI experiment where a methanol solution of the amino alcohol ligand was sprayed onto a surface containing the *p*-cymene Ru dimer $[(p\text{-cymene})\text{RuCl}_2]_2$.⁷⁰

To analyze the Ru complexes after electrocatalysis, a sample of complex **2** supported on EPG was immersed in an aqueous solution containing 1.23 M MeOH, 0.1 M sodium perchlorate, and 0.01 M phosphate buffer at pH 11.5 and subjected to a series of rotating disk electrode voltammograms from 200 to 1200 mV vs NHE, exactly as done for the electrocatalytic kinetics analysis. The electrode was removed from the solution, allowed to dry in air, and analyzed by DESI by spraying degassed methanol onto the electrode. The DESI spectrum shown in Figure 4b reveals that the major ion observed is that at m/z 384.0907, corresponding to the cation $2a^+$. The ion at m/z 420.0667 corresponding to **2** decreased significantly in abundance (Figure 4b), implicating that most of the Ru–Cl precursor is consumed during electrocatalysis. Notably, the peaks at m/z 689.04300 and 838.1272 are no longer observed, suggesting that the chlorides are displaced during the course of the experiment. The observation that $2a^+$ is observed as the major species following electrooxidation (Figure 4b) implies that a significant fraction of the Ru complexes on the surface retain both the cymene ligand and the amino alcohol ligand under an applied potential. This experiment attests to the stability of the complex **2a** under the electrocatalytic conditions, though it does not allow us to infer that **2a** is the active catalyst.

Additionally, several minor species detected in the DESI mass spectrum could be assigned unambiguously (Figures 4 and 5; errors were <3.5 ppm and at least three of the most intense peaks of the isotope distribution were observed in the mass spectrum).⁷¹ We assign the ion at m/z 424.0826 to the $\text{Ru}^{\text{II}}\text{--OH}$ species $2d\text{Na}^+$ (0.71 ppm) (Figure 4c) and that at m/z 482.0881 to the $\text{Ru}^{\text{IV}}\text{--methoxy formate}$ species $2e^+$ (1.0 ppm) (Figure 4d). Also identified, albeit in very low abundance, were species assigned as the $\text{Ru}^{\text{II}}\text{--formic acid adduct}$ $2f^+$ at m/z 430.09556 (2.6 ppm) and $\text{Ru}^{\text{IV}}\text{--hydroxy formate}$ species $2g^+$ at m/z 446.0900 (3.4 ppm) (Figures S20 and S21, Supporting Information). This information provides indirect evidence for the formation of these Ru species on the EPG electrode surface under an applied potential. Although these ions were observed on the electrode surface following the electrochemistry experiments, we cannot completely exclude the possibility that they were formed in the DESI experiment in the secondary microdroplets. However, significantly, this technique enables one to obtain information not possible to collect by any other means.

Catalytic transfer hydrogenation experiments reveal that the chemical oxidation product of methanol by **2** is methyl formate.³¹ Moreover, our DESI studies on the EPG electrodes

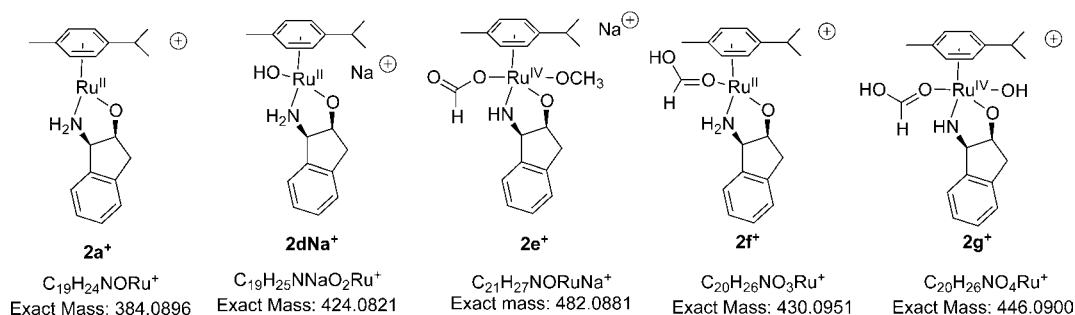


Figure 5. Ions observed on the edge-plane graphite electrode following electrocatalysis.

have identified species containing formic acid or formate subsequent to the electrocatalytic process that were not present in the absence of an applied potential (Figures 4 and 5). No masses were observed corresponding to proposed Ru–CO or Ru–CO₂ species. This evidence indicates that the Ru cymene complexes **1** and **2** serve as active precursors for the electrocatalytic oxidation of methanol to formate.

CONCLUSIONS

Ruthenium arene transfer hydrogenation complexes are active electrocatalytic precursors for alcohol oxidation when supported on edge-plane graphite electrodes in basic aqueous solution. Amino alcohol chloride **2** exhibits a rate of approximately 1 turnover/s for methanol electrooxidation by four electrons at 750 mV vs NHE with an onset of electrocatalytic current at 560 mV vs NHE. The use of DESI-MS experiments on electrode surfaces and ¹H NMR experiments imply that **2** is capable of oxidizing methanol by four electrons to formate species. The Nernstian dependence on the anodic peak potential in the CV of **2** on EPG coupled with the slow rates of TH for **2** and the relatively high potentials required for observation of electrocatalysis (ca. 1.2 V above the thermodynamic oxidation potential of methanol to formate) lead us to conclude that the electrocatalytic oxidation of methanol to formate by **2** on edge-plane graphite electrodes in water is mediated by Ru=O species rather than Ru–H species.

ASSOCIATED CONTENT

Supporting Information

Text and figures giving experimental methods, NMR spectra, cyclic voltammetry, mass spectra, synthesis details, and characterization data. This material is available free of charge via the Internet at <http://pubs.acs.org>.

AUTHOR INFORMATION

Corresponding Author

waymouth@stanford.edu.

Notes

The authors declare no competing financial interest.

ACKNOWLEDGMENTS

We acknowledge the NSF (CHE-1213403) and the Global Climate and Energy Program at Stanford. R.H.P. and R.N.Z. thank the Air Force Office of Scientific Research for support of this project under AFOSR FA9550-10-1-0235. K.B. thanks the Center for Molecular Analysis and Design (CMAD) at Stanford for a graduate fellowship; C.C.L.M. thanks the Ford Foundation for a Dissertation Fellowship. We also thank Pavel Aronov and Allis Chien (Stanford University Mass Spectrometry) for providing mass spectrometry instrumentation.

REFERENCES

- (1) Olah, G. A. *Angew. Chem., Int. Ed. Engl.* **2005**, *44*, 2636–2639.
- (2) Rabis, A.; Rodriguez, P.; Schmidt, T. J. *ACS Catal.* **2012**, *2*, 864–890.
- (3) Krewer, U.; Vidakovic-Koch, T.; Rihko-Struckmann, L. *ChemPhysChem* **2011**, *12*, 2518–2544.
- (4) Bianchini, C.; Shen, P. K. *Chem. Rev.* **2009**, *109*, 4183–4206.
- (5) Gurau, B.; Viswanathan, R.; Liu, R.; Lafrenz, T. J.; Ley, K. L.; Smotkin, E. S.; Reddington, E.; Sapienza, A.; Chan, B. C.; Mallouk, T. E.; Sarangapani, S. *J. Phys. Chem. B* **1998**, *102*, 9997–10003.

- (6) Liu, H.; Song, C.; Zhang, L.; Zhang, J.; Wang, H.; Wilkinson, D. P. *J. Power Sources* **2006**, *155*, 95–110.
- (7) Hori, Y. *Mod. Aspects Electrochem.* **2008**, *42*, 89–189.
- (8) Fachini, E. R.; Diaz-Ayala, R.; Casado-Rivera, E.; File, S.; Cabrera, C. R. *Langmuir* **2003**, *19*, 8986–8993.
- (9) Annen, S. P.; Bambagioni, V.; Bevilacqua, M.; Filippi, J.; Marchionni, A.; Oberhauser, W.; Schönberg, H.; Vizza, F.; Bianchini, C.; Grützmaier, H. *Angew. Chem., Int. Ed.* **2010**, *49*, 7229–7233.
- (10) Bevilacqua, M.; Bianchini, C.; Marchionni, A.; Filippi, J.; Lavacchi, A.; Miller, H.; Oberhauser, W.; Vizza, F.; Granozzi, G.; Artiglia, L.; Annen, S. P.; Krumeich, F.; Grützmaier, H. *Energy Environ. Sci.* **2012**, *5*, 8608–8620.
- (11) Elouarzaki, K.; Le Goff, A.; Holzinger, M.; Thery, J.; Cosnier, S. *J. Am. Chem. Soc.* **2012**, *134*, 14078–14085.
- (12) Meyer, T. J.; Huynh, M. H. V. *Inorg. Chem.* **2003**, *42*, 8140–8160.
- (13) Cheung, K.-C.; Wong, W.-L.; Ma, D.-L.; Lai, T.-S.; Wong, K.-Y. *Coord. Chem. Rev.* **2007**, *251*, 2367–2385.
- (14) Hu, Z.; Du, H.; Leung, C.-F.; Liang, H.; Lau, T.-C. *Ind. Eng. Chem. Res.* **2011**, *50*, 12288–12292.
- (15) Kutner, W.; Meyer, T. J.; Murray, R. W. *J. Electroanal. Chem.* **1985**, *195*, 375–394.
- (16) Li, C. K.; Tang, W. T.; Che, C. M.; Wong, K. Y.; Wang, R. J.; Mak, T. C. W. *J. Chem. Soc., Dalton Trans.* **1991**, 1909–1914.
- (17) Lai, Y. K.; Wong, K. Y. *Electrochim. Acta* **1993**, *38*, 1015–1021.
- (18) Gerli, A.; Reedijk, J.; Lakin, M. T.; Spek, A. L. *Inorg. Chem.* **1995**, *34*, 1836–1843.
- (19) Hornstein, B. J.; Dattelbaum, D. M.; Schoonover, J. R.; Meyer, T. J. *Inorg. Chem.* **2007**, *46*, 8139–8145.
- (20) Gladiali, S.; Alberico, E. *Chem. Soc. Rev.* **2006**, *35*, 226–236.
- (21) Ikariya, T.; Blacker, A. J. *Acc. Chem. Res.* **2007**, *40*, 1300–1308.
- (22) Haack, K. J.; Hashiguchi, S.; Fujii, A.; Ikariya, T.; Noyori, R. *Angew. Chem., Int. Ed.* **1997**, *36*, 285–288.
- (23) Hashiguchi, S.; Fujii, A.; Haack, K. J.; Matsumura, K.; Ikariya, T.; Noyori, R. *Angew. Chem., Int. Ed.* **1997**, *36*, 288–290.
- (24) Ikariya, T.; Murata, K.; Noyori, R. *Org. Biomol. Chem.* **2006**, *4*, 393–406.
- (25) Matsumura, K.; Hashiguchi, S.; Ikariya, T.; Noyori, R. *J. Am. Chem. Soc.* **1997**, *119*, 8738–8739.
- (26) Noyori, R.; Yamakawa, M.; Hashiguchi, S. *J. Org. Chem.* **2001**, *66*, 7931–7944.
- (27) Takehara, J.; Hashiguchi, S.; Fujii, A.; Inoue, S.-i.; Ikariya, T.; Noyori, R. *Chem. Commun.* **1996**, 233–234.
- (28) Palmer, M.; Walsgrove, T.; Wills, M. J. *Org. Chem.* **1997**, *62*, 5226–5228.
- (29) Kenny, J. A.; Wills, M.; Versluis, K.; Heck, A. J. R.; Walsgrove, T. *Chem. Commun.* **2000**, 99–100.
- (30) Blacker, J.; Martin, J. *Asymmetric Catalysis on Industrial Scale*; Wiley: New York, 2004.
- (31) Perry, R. H.; Brownell, K. R.; Chingin, K.; Cahill, T. J.; Waymouth, R. M.; Zare, R. N. *Proc. Natl. Acad. Sci. U.S.A.* **2012**, *109*, 2246–2250.
- (32) Smith, T. A.; Aplin, R. P.; Maitlis, P. M. *J. Organomet. Chem.* **1985**, *291*, C13–C14.
- (33) Yang, L. C.; Ishida, T.; Yamakawa, T.; Shinoda, S. *J. Mol. Catal. A: Chem.* **1996**, *108*, 87–93.
- (34) Pearson, D. M.; Waymouth, R. M. *Organometallics* **2009**, *28*, 3896–3900.
- (35) Nishimura, T.; Kakiuchi, N.; Onoue, T.; Ohe, K.; Uemura, S. *J. Chem. Soc., Perkin Trans. 1* **2000**, 1915–1918.
- (36) Nielsen, M.; Alberico, E.; Baumann, W.; Drexler, H. J.; Junge, H.; Gladiali, S.; Beller, M. *Nature* **2013**, *495*, 85–89.
- (37) Thompson, M. S.; Meyer, T. J. *J. Am. Chem. Soc.* **1982**, *104*, 4106–4115.
- (38) Llobet, A. *Inorg. Chim. Acta* **1994**, *221*, 125–131.
- (39) Bard, A. J.; Faulkner, L. R. *Electrochemical Methods: Fundamentals and Applications*, 2nd ed.; Wiley: New York, 2001.
- (40) Brownell, K. B.; Waymouth, R. M. Manuscript in preparation.

- (41) Bambagioni, V.; Bianchini, C.; Marchionni, A.; Filippi, J.; Vizza, F.; Teddy, J.; Serp, P.; Zhiani, M. *J. Power Sources* **2009**, *190*, 241–251.
- (42) Raoof, J.-B.; Ojani, R.; Hosseini, S. R. *J. Power Sources* **2011**, *196*, 1855–1863.
- (43) Zheng, L.; Song, J.-f. *J. Solid State Electrochem.* **2010**, *14*, 43–50.
- (44) Chan, S. L.-F.; Kan, Y.-H.; Yip, K.-L.; Huang, J.-S.; Che, C.-M. *Coord. Chem. Rev.* **2011**, *255*, 899–919.
- (45) Che, C.-M.; Cheng, K.-W.; Chan, M. C. W.; Lau, T.-C.; Mak, C.-K. *J. Org. Chem.* **2000**, *65*, 7996–8000.
- (46) Che, C.-M.; Ho, C.; Lau, T.-C. *J. Chem. Soc., Dalton Trans.* **1991**, 1901–1907.
- (47) Che, C.-M.; Yip, W.-P.; Yu, W.-Y. *Chem. Asian J.* **2006**, *1*, 453–458.
- (48) Laurent, F.; Plantalech, E.; Donnadiou, B.; Jimenez, A.; Hernandez, F.; Martinez-Ripoll, M.; Biner, M.; Llobet, A. *Polyhedron* **1999**, *18*, 3321–3331.
- (49) Sens, C.; Rodriguez, M.; Romero, I.; Llobet, A. *Inorg. Chem.* **2003**, *42*, 8385–8394.
- (50) Rodriguez, M.; Romero, I.; Llobet, A.; Deronzier, A.; Biner, M.; Parella, T.; Stoeckli-Evans, H. *Inorg. Chem.* **2001**, *40*, 4150–4156.
- (51) Roecker, L.; Meyer, T. J. *J. Am. Chem. Soc.* **1987**, *109*, 746–754.
- (52) *Standard Potentials in Aqueous Solution*, 1st ed.; Bard, A. J., Parsons, R., Jordan, J., Eds.; Marcel Dekker: New York, 1985.
- (53) Ozawa, H.; Hino, T.; Ohtsu, H.; Wada, T.; Tanaka, K. *Inorg. Chim. Acta* **2011**, *366*, 298–302.
- (54) Serra, D.; Correia, M. C.; McElwee-White, L. *Organometallics* **2011**, *30*, 5568–5577.
- (55) Paul, A.; Hull, J. F.; Norris, M. R.; Chen, Z.; Ess, D. H.; Concepcion, J. J.; Meyer, T. J. *Inorg. Chem.* **2011**, *50*, 1167–1169.
- (56) Hembre, R. T.; McQueen, J. S.; Day, V. W. *J. Am. Chem. Soc.* **1996**, *118*, 798–803.
- (57) Romming, C.; Smith, K.-T.; Tilset, M. *Inorg. Chim. Acta* **1997**, *259*, 281–290.
- (58) Wu, X.; Liu, J.; Di Tommaso, D.; Iggo, J. A.; Catlow, C. R. A.; Bacsá, J.; Xiao, J. *Chem. Eur. J.* **2008**, *14*, 7699–7715.
- (59) Muller, J. G.; Acquaye, J. H.; Takeuchi, K. *J. Inorg. Chem.* **1992**, *31*, 4552–4557.
- (60) Sala, X.; Poater, A.; Romero, I.; Rodríguez, M.; Llobet, A.; Solans, X.; Parella, T.; Santos, T. M. *Eur. J. Inorg. Chem.* **2004**, *2004*, 612–618.
- (61) Thai, T.-T.; Therrien, B.; Süß-Fink, G. *J. Organomet. Chem.* **2011**, *696*, 3285–3291.
- (62) Singh, P.; Singh, A. K. *Organometallics* **2010**, *29*, 6433–6442.
- (63) Huynh, M. H. V.; Meyer, T. J. *Chem. Rev.* **2007**, *107*, 5004–5064.
- (64) Moyer, B. A.; Meyer, T. J. *Inorg. Chem.* **1981**, *20*, 436–444.
- (65) Cooks, R. G.; Ouyang, Z.; Takats, Z.; Wiseman, J. M. *Science* **2006**, *311*, 1566–1570.
- (66) Takats, Z.; Wiseman, J. M.; Cooks, R. G. *J. Mass Spectrom.* **2005**, *40*, 1261–1275.
- (67) Takats, Z. W.; Wiseman, J. M.; Gologan, B.; Cooks, R. G. *Science* **2004**, *306*, 471–473.
- (68) Perry, R. H.; Splendore, M.; Chien, A.; Davis, N. K.; Zare, R. N. *Angew. Chem., Int. Ed.* **2011**, *50*, 250–254.
- (69) Liu, P.; Lanekoff, I. T.; Laskin, J.; Dewald, H. D.; Chen, H. *Anal. Chem.* **2012**, *84*, 5737–5743.
- (70) Ions corresponding to the cationic dimer (m/z 576.9340) and dimer $[2+2]^+$ (m/z 838.1272) are likely formed in the secondary microdroplets after **2** is extracted from the surface, consistent with the conclusions of our recent communication.³¹
- (71) Several additional ions were observed that could not be readily assigned.